

Published in final edited form as:

*Biomaterials*. 2013 September ; 34(28): 6572–6579. doi:10.1016/j.biomaterials.2013.05.048.

## Co-encapsulation of anti-BMP2 monoclonal antibody and mesenchymal stem cells in alginate microspheres for bone tissue engineering

Alireza Moshaverinia, DDS, MS, PhD<sup>1,§</sup>, Sahar Ansari, MSc<sup>2,§</sup>, Chider Chen, MSc<sup>1</sup>, Xingtian Xu, DDS<sup>1</sup>, Kentaro Akiyama, DDS, PhD<sup>1</sup>, Malcolm L. Snead, DDS, PhD<sup>1</sup>, Homayoun H. Zadeh, DDS, PhD<sup>2,\*</sup>, and Songtao Shi, DDS, PhD<sup>1</sup>

<sup>1</sup>Center for Craniofacial Molecular Biology, Ostrow School of Dentistry of USC, University of Southern California, Los Angeles, CA

<sup>2</sup>Laboratory for Immunoregulation and Tissue Engineering (LITE), Ostrow School of Dentistry of USC, University of Southern California, Los Angeles, CA

### Abstract

Recently, it has been shown that tethered anti-BMP2 monoclonal antibodies (mAbs) can trap BMP ligands and thus provide BMP inductive signals for osteo-differentiation of progenitor cells. The objectives of this study were to: (1) develop a co-delivery system based on murine anti-BMP2 mAb-loaded alginate microspheres encapsulating human bone marrow mesenchymal stem cells (hBMMSCs); and (2) investigate osteogenic differentiation of encapsulated stem cells in alginate microspheres *in vitro* and *in vivo*. Alginate microspheres of  $1 \pm 0.1$  mm diameter were fabricated with  $2 \times 10^6$  hBMMSCs per mL of alginate. Critical-size calvarial defects (5 mm diameter) were created in immune-compromised mice and alginate microspheres preloaded with anti-BMP mAb encapsulating hBMMSCs were transplanted into defect sites. Alginate microspheres pre-loaded with isotype-matched non-specific antibody was used as the negative control. After 8 weeks, micro CT and histologic analysis were used to analyze bone formation. *In vitro* analysis demonstrated that anti-BMP2 mAbs tethered BMP2 ligands that can activate the BMP receptors on hBMMSCs. The co-delivery system described herein, significantly enhanced hBMMSC-mediated osteogenesis, as confirmed by the presence of BMP signal pathway-activated osteoblast determinants Runx2 and ALP. Our results highlight the importance of engineering the microenvironment for stem cells, and particularly the value of presenting inductive signals for osteo-differentiation of hBMMSCs by tethering BMP ligands using mAbs. This strategy of engineering the microenvironment with captured BMP signals is a promising modality for repair and regeneration of craniofacial, axial and appendicular bone defects.

© 2013 Elsevier Ltd. All rights reserved.

\*Corresponding Author: Homayoun H. Zadeh, DDS, PhD, Associate Professor, Director, Post-Doctoral Periodontology Program, Laboratory for Immunoregulation & Tissue Engineering, Herman Ostrow School of Dentistry, University of Southern California, 925 West 34th Street, Los Angeles, CA 90089, USA. Tel.: + 1 213 740 1415. Fax: + 1 213 740 2194. zadeh@usc.edu.

§These authors contributed equally to this work.

The authors declare no potential conflicts of interest with respect to the authorship and/or publication of this article.

**Publisher's Disclaimer:** This is a PDF file of an unedited manuscript that has been accepted for publication. As a service to our customers we are providing this early version of the manuscript. The manuscript will undergo copyediting, typesetting, and review of the resulting proof before it is published in its final citable form. Please note that during the production process errors may be discovered which could affect the content, and all legal disclaimers that apply to the journal pertain.

## Keywords

Alginate hydrogel; Mesenchymal stem cell-mediated bone regeneration; Cells encapsulation; Anti-BMP2 monoclonal antibodies

---

## 1. Introduction

Currently, reconstruction of missing or damaged bone can be accomplished by an array of surgical procedures [1,2]. Autologous bone has been considered the “gold standard” for bone augmentation. Autologous and allogenic bone grafts currently comprise more than 90% of grafts performed each year [3,4]. However, there are several disadvantages associated with this methodology, such as donor site morbidity, hematoma, inflammation, and the high cost of bone harvesting procedures [5,6]. The ultimate goal of bone tissue engineering is the fabrication of a construct that matches the physical and biological properties of the natural bone tissue, without the drawbacks imposed by autologous or allogenic bone grafts. The extensive distribution of stem cells in many adult tissues, with their ability to give rise to multiple specialized cell types, has made them an attractive target for applications in tissue engineering. Mesenchymal stem cells (MSCs), such as human bone marrow mesenchymal stem cells (hBMMSCs), can differentiate into one of many cell lineages, including craniofacial bone osteoblasts, depending on the nature of the environmental signals that they receive [7-9]. Both preclinical and clinical studies have shown the application of hBMMSCs to be a promising treatment modality for generating new bone through stem cell-mediated bone tissue engineering [10-12].

To guide the differentiation of hBMMSC, it may be necessary and desirable to deliver an appropriate signal that is specific to the desired lineage/phenotype, and hence, exogenous growth factors have been delivered along with stem cells. It is well known that stem cell-mediated bone regeneration is partially controlled by the recipient local microenvironment, including the presence of growth factors, immune cells and cytokines [13-16]. However, there are a number of limitations to the application of exogenous growth factors, including significant side effects, reduced efficacy compared to endogenous counterparts, high cost, difficulty of achieving optimal kinetics for delivery, and temporal and spatial requirements for their availability [16-19]. As an alternative to using recombinant human bone morphogenetic protein 2 (rhBMP2) as an exogenous growth factor, investigators have recently shown the ability of specific monoclonal antibodies (mAb) directed against BMP2 to capture endogenous BMP2 ligands from the engraftment site and present them to progenitor stem cells, promoting bone repair and regeneration [20, 21]. Therefore, one can envision that combining the stem cells with antibodies selected for their capacity to capture therapeutic ligands could enhance the quality and quantity of stem cell-mediated bone regeneration.

In addition, it is also well known that the cell delivery vehicle helps to dictate the success of regenerative therapy by improving the *in vivo* performance of stem cells. Several types of scaffolds have been used to support growth and differentiation of progenitor cells for bone regeneration, including natural polymers such as alginates. In previous studies, we have utilized alginate hydrogels as a scaffold for the encapsulation of dental-derived adult MSCs [23,24]. Alginates are natural hetero-polysaccharides with unique properties, including gentle gelation behavior, biodegradability, biocompatibility, ease of cell encapsulation/cell recovery, and chemical versatility, making them useful for the encapsulation of cells and bioactive molecules that can be used to facilitate minimally invasive surgical procedures [38-40]. Therefore, in seeking a platform for bone tissue engineering, we chose to utilize an RGD-coupled alginate hydrogel as the scaffold for the simultaneous encapsulation of

hBMMSCs with an anti-BMP2 mAb to capture endogenous BMP2 growth factor. We hypothesized that this combination of vehicle, MSCs, and mAbs would provide an effective method for improving the osteogenic differentiation of these stem cells.

## 2. Materials and Methods

### 2.1. Antibodies

We used clone 3G7, a mouse anti-BMP2 IgG2 monoclonal antibody (mAb) (Abnova, Taipei, Taiwan). An isotype-matched mAb (Iso mAb) with no specificity for BMP2 was utilized as the negative control.

### 2.2. Stem cell culture and flow cytometry analysis

Human bone marrow mesenchymal stem cells (hBMMSCs), processed from marrow aspirates of normal human adult volunteers (20–35 years of age) according to a previously published method [22], were purchased from Poietic Technologies (Gaithersburg, MD). hBMMSCs were cultured in  $\alpha$ -MEM (Invitrogen, Grand Island, NY) supplemented with 15% Fetal Bovine Serum (FBS, Invitrogen, San Diego CA), 100 units/mL penicillin (Invitrogen), and 100  $\mu$ g/mL streptomycin (Invitrogen). Passage four cells were used for all experiments.

To characterize the specificity of our murine anti-BMP2 mAb (3G7), hBMMSCs were cultured and analyzed by flow cytometry. This procedure evaluated the presence or absence of an immune complex formed between the anti-BMP2 mAb and the BMP2 ligand that binds with the BMP2 receptor on hBMMSCs. Recombinant human bone morphogenetic protein (rhBMP2, Medtronic, Minneapolis, MN) was used as a growth factor standard. Briefly, rhBMP2 (100 ng/mL) was incubated with anti-BMP2 mAb (25  $\mu$ g/mL) for 30 min at 4°C and the resulting immune complex was incubated with hBMMSCs. The immune complex was immunofluorescently detected using phycoerythrin-conjugated goat anti-mouse Ab (Becton Dickinson, Franklin Lakes, NJ). The intensity of fluorescent labeling was determined by measuring the mean fluorescent intensity (MFI) with a flow cytometer (FACS Calibur; Becton Dickinson). The experiment was repeated using an type-matched non-specific mAb (Iso mAb) as the negative control.

### 2.3. In vitro osteogenic differentiation

To study the effects of anti-BMP2 mAb on osteogenesis of hBMMSCs *in vitro*,  $1 \times 10^5$  hBMMSCs were cultured in 6-well plates in culture media containing  $\alpha$ -MEM (Invitrogen), 15% FBS (Invitrogen), 100 units/mL penicillin (Invitrogen), and 100  $\mu$ g/mL streptomycin (Invitrogen); and supplemented in one of the following ways: (1) recombinant human BMP2 (rhBMP2) at 100 ng/mL, serving as a positive control; (2) anti-BMP2 mAb (25  $\mu$ g/mL) + rh-BMP2 (100 ng/mL); (3) non-specific isotype mAb (25  $\mu$ g/mL) + rhBMP2 (100 ng/mL), serving as an antibody control; and 4) no further supplementation, serving as a treatment control. The culture dishes were first coated with either mAb or non-specific isotype mAb to immobilize the mAbs, non-specific binding sites were blocked with bovine serum albumin (0.5 mg/mL BSA, Invitrogen), and rh-BMP2 was added. After allowing 60 minutes for the rh-BMP2 ligand to bind, the dishes were washed thoroughly with PBS to remove free rh-BMP2 ligand. The medium was changed twice per week.

After two weeks in culture, the differentiation of the hBMMSCs was analyzed using Alizarin red staining. Briefly, hBMMSC cultures were washed twice with PBS, fixed for 1 min in 60% isopropanol, and rehydrated with distilled water. They were then stained with Alizarin red S dye solution for 5 min and excess dye was removed by washing twice with deionized water. Retained Alizarin red S was quantified using NIH ImageJ software

(Version 1.64, NIH, Bethesda, MD) by determining the area positive for dye staining expressed as a fraction of the total area.

After two weeks in culture, the differentiation of hBMMSCs was analyzed using Western blot analysis. Briefly, the cells were washed twice with PBS and lysed with protein extraction buffer (Bio-Rad, Irvine, CA) for 30 sec. The supernatant was cleared by centrifugation and the protein concentration was determined using a BCA assay (Pierce, Rockford, IL) by extrapolation to a known BSA standard concentration by serial dilution across one order of magnitude. Equal amounts of protein extracts were fractionated to size by electrophoresis in 10% sodium dodecyl sulfate-polyacrylamide gels (PAGE), and the size-resolved proteins were electrophoretically transferred to a nitrocellulose membrane (Bio-Rad). The nitrocellulose membrane was incubated with rabbit antibody directed against phospho-Smad1 (Santa Cruz Biotechnology, Dallas, TX) or Runx2 (Abcam, Cambridge, MA). Immune-protein complexes were detected using a secondary antibody at 1:500 (polyclonal goat anti-rabbit IgG/HRP, EMD Millipore, Billerica, MA). The membranes were stripped and re-probed with an antibody directed against the housekeeping gene beta-actin (Abcam) to ensure that equal mass was loaded to each lane. The chemiluminescent reagent (Amersham Life Science, Pittsburgh, PA) was added to the membrane for 1 min and exposed to x-ray film for variable periods (Thermo Scientific, Rockford, IL) to produce images.

A colorimetric p-nitrophenyl phosphate assay (Abcam) was utilized to measure the alkaline phosphatase (ALP) activity of hBMMSCs in the culture conditions described above. The cells were washed three times with PBS, collected by centrifugation, lysed, and then the ALP reaction buffer was added to each sample. The level of ALP activity was normalized to the amount of total DNA in each of the cell lysates. Normal control serum (Stanbio, Boerne, TX) containing a known ALP concentration was used as a standard for extrapolation of unknown values.

#### 2.4. Biomaterial fabrication and cell encapsulation

Custom-made RGD-coupled alginate with high glucouronic acid content ((NovaMatrix FMC Biopolymer, Norway) was utilized in this study. The RGD-coupled alginate was purified and partially oxidized (5%) to increase its degradability according to published methods [23, 24]. Subsequently, the alginate was mixed with anti-BMP2 mAb (25  $\mu\text{g}/\text{mL}$ ) or control non-specific isotype mAb by vigorous stirring.

hBMMSCs at a density of  $2 \times 10^6$  cells per mL of alginate solution were encapsulated in RGD-coupled alginate loaded with either mAb or non-specific Iso mAb. Formation of microspheres was accomplished by extruding droplets of the alginate mixture through a syringe into a solution of 100 mM calcium chloride. The microspheres were incubated at 37°C for 45 min and washed three times in DMEM without supplements.

#### 2.5. In vitro release kinetics study

The kinetics of mAb release from alginate microspheres was evaluated by suspending the mAb-loaded alginate microspheres in 50 mL of PBS (pH=7.4). At various time points (1, 3, 7, and 14 days), the amount of released mAb was determined by UV absorption spectroscopy (Beckman, Brea CA). Retained mAb was detected with FITC-conjugated goat anti-mouse IgG antibody (Santa Cruz Biotechnology Inc, CA) and measured using confocal laser scanning microscopy (CLSM).

## 2.6. Human BMMSC-mediated antibody assisted bone regeneration in vivo

The USC Institutional Animal Care and Use Committee approved all procedures involving vertebrate animals. Human BMMSCs were encapsulated in anti-BMP2 mAb-loaded alginate hydrogel microspheres and transplanted into a 5 mm diameter critical size calvarial defect in 5-month-old Beige nude *XID III (NU/NU)* mice (Harlan Laboratories, Livermore, CA). Immunocompromised mice were selected to avoid immunogenic and graft-rejection responses due to the human origin of the stem cells.

A total of 20 *NU/NU* mice were used as hosts and had calvarial defects treated in one of the following ways: encapsulated hBMMSCs (n=4); encapsulated hBMMSCs + anti-BMP2 mAb (25 µg/mL) (n=4); alginate microspheres + anti-BMP2 mAb (n=4); alginate microspheres + rhBMP2 (25 µg/mL) (n=4); alginate microspheres + non-specific isotype mAb (n=4). Animals were sacrificed 8 weeks after transplantation.

## 2.7. Micro-CT Analysis

Upon sacrifice at 8 weeks following transplantation, the calvarial defects were examined using a high-resolution micro CT system (MicroCAT II, Siemens Medical Solutions Molecular Imaging, Knoxville, TN) to evaluate the healing of the defects. The specimens were scanned every 10 µm at 60 kV and 110 µA at a spatial resolution of 18.7 µm (Voxel dimension) and three-dimensional (3D) histomorphometric analysis was performed on the resulting images. Bone volume fraction divided by total volume (BV/TV) of newly regenerated bone for each stem cell-alginate construct was calculated using Amira software (Visage Imaging Inc. San Diego CA).

## 2.8. Histology, immunohistochemical and immunofluorescent staining

For histological examination, specimens were fixed in 10% formalin solution and decalcified with 10% EDTA for four weeks. Samples were dehydrated in an ascending series of ethanol and embedded in paraffin. Sections of 6 µm thickness were prepared using a microtome and mounted on subbed glass slides. Four randomly selected cross sections from each implant were stained with hematoxylin and eosin (H&E) or Masson's Trichrome stains.

To identify the origin of the cells, paraffin-embedded sections were incubated with a primary antibody directed against human mitochondria (Chemicon, Billerica, MA) at 1:200 dilution and the immune complex was detected using an immunoperoxidase ABC kit (HRP, Vector Laboratories, Burlingame, CA). Sections were counterstained with hematoxylin.

For immunohistochemical analysis, de-paraffinized sections were washed, and non-specific endogenous peroxidase activity was quenched by immersing in 3% H<sub>2</sub>O<sub>2</sub>/methanol for 15 min. Sections were incubated with primary antibody (1:200–1:300 dilution) for 1 h. Immunohistochemistry examination was performed on sections using anti-Runx2 (Santa Cruz Biotechnology, 1:100 dilution) and anti-BMP2 (Abcam, 1:200 dilution) and counterstaining with hematoxylin.

## 2.9. Statistical analysis of data

Quantitative data were expressed as mean ± standard deviation (SD). One-way and two-way analyses of variance (ANOVA) followed by Tukey's test at a significance level of  $\alpha = 0.05$  were used for the comparison among multiple sample means.

### 3. Results

#### 3.1 Binding of BMP-2/Anti-BMP2 immune complex to hBMSCs

In order to assess the ability of the immune complex formed between the murine anti-BMP2 mAb and rhBMP2 ligand to bind with the hBMSC BMP-2 cellular receptor, an *in vitro* flow cytometric analysis was utilized. Flow cytometric analysis confirmed significant binding of hBMSC receptors with the anti-BMP-2 mAb and BMP2 ligand immune complex (Fig. 1a). Negative controls consisting of non-specific isotype-matched mAb (Iso mAb) or hBMSCs alone showed no binding.

#### 3.2. Osteogenic differentiation of hBMSCs *in vitro* in the presence of anti-BMP2 mAb

An *in vitro* model was developed to evaluate the effect of the anti-BMP2 mAb + rhBMP2 immune complex on the differentiation of stem cells. hBMSCs were cultured in four different conditions: 1) rhBMP2 (positive control); 2) anti-BMP2 mAb + rhBMP2 immune complex; 3) Non-specific Iso mAb (negative control); and 4) media alone without supplementation (negative control). The osteogenic differentiation of hBMSCs was analyzed using Alizarin red S staining. After 2 weeks, hBMSCs from the positive control and experimental groups both differentiated into positive Alizarin red S staining nodules, indicative of their osteogenic fate (Fig. 1b), while neither of the two negative control groups exhibited positive Alizarin red S dye staining. As expected, no statistically significant difference ( $p>0.05$ ) was found between cells cultured in the presence of rhBMP2 ligand alone and those cultured with the immune complex formed by anti-BMP2 mAb + rhBMP2 ligand, supporting the interpretation that the immune complex of anti-BMP2 mAb + rhBMP2 ligand actively binds to BMP receptors located on the hBMSCs and contributes to their osteogenic differentiation (Fig. 1b). The results from our Western blot analysis correlated well with the data from the histochemical staining. Increased expression levels for the osteoblastic-specific molecule, Runx2, were detected in specimens cultured for two weeks in the presence of anti-BMP2 mAb + rhBMP2 ligand immune complex (Fig. 1c). Similarly, cells cultured in the presence of anti-BMP2 mAb + rhBMP2 ligand immune complex revealed up-regulation of phospho-Smad1. In contrast, cells maintained in the presence of non-specific isotype mAb failed to activate the BMP signaling pathway, as shown by their very modest levels of phospho-Smad1 and Runx2 expression.

The ALP activity levels observed for hBMSCs maintained in different culture conditions are presented in Figure 1d. High levels of ALP activity were observed for hBMSCs, both in the presence of rhBMP2 ligand alone and in the presence of anti-BMP2 mAb + rhBMP2 ligand immune complex, manifesting peak activity during the second week of culture. However, no statistically significant difference was observed in the amount of ALP activity between cells treated with the BMP2 ligand alone or the anti-BMP2 mAb + rhBMP2 immune complex at any time interval examined ( $p>0.05$ ). In contrast, only modest ALP activity was observed for the cells grown in either medium alone or with non-specific isotype mAb ( $p<0.01$ ).

#### 3.3. Development and characterization of stem cell-based delivery system to improve bone tissue regeneration

Here, we describe the design of a system for encapsulating MSCs in RGD-alginate microspheres with an average diameter of 1mm (Fig 2a). Microscopic images of stem cell-loaded microspheres revealed a uniform cell distribution (Fig. 2b). The design was enhanced by the incorporation of anti-BMP2 mAb (25  $\mu\text{g}/\text{mL}$ ) via absorption during the creation of the microspheres. The release profile of mAb from the alginate microspheres showed sustained release for up to 14 days (Fig. 2c). Moreover, the microspheres still retained anti-

BMP2 mAb after 14 days, as revealed by immunofluorescent staining with an FITC-conjugated goat anti-mouse IgG antibody (Fig. 2d).

### 3.4. Human BMMSCs and mAb contributed to bone regeneration in a critical size calvarial defect model

We hypothesized that stem cell-mediated bone regeneration could be enhanced with the addition of therapeutic antibodies to attract and tether host-derived BMP ligands, and that such an integrated system would constitute a promising platform for bone tissue engineering due to its ability to modulate the BMP signaling pathway. In order to test this platform, we applied mAb-loaded RGD-alginate microspheres with  $2 \times 10^6$  encapsulated hBMMSCs into 5 mm critical-sized calvarial defects in immune-compromised mice. Samples consisting of encapsulated hBMMSCs alone in alginate or rhBMP2 alone in alginate were used as the positive controls, while alginate loaded with non-specific isotype mAb was used as the negative control. The quantity and quality of bone regenerated in the calvarial defect sites were evaluated after 8 weeks using micro-CT and histological analyses. Micro-CT analysis (Fig. 3a) demonstrated the greatest amounts of bone repair in the experimental group, which received alginate hydrogel containing anti-BMP2 mAb and encapsulated hBMMSCs. Quantitative analysis of the micro-CTs showed that the positive control groups (e.g. encapsulated hBMMSCs and encapsulated anti-BMP2 mAb) formed less bone than the experimental group that combined the anti-BMP2 mAb with encapsulated hBMMSCs ( $p < 0.05$ ) (Fig. 3b). The negative control group regenerated the smallest amount of bone of all the groups during the experimental period ( $p < 0.05$ ).

Histological evidence supported the micro-CT observations demonstrating that the hBMMSC-mediated, mAb-assisted concept significantly increased the amount of bone tissue formed within the critical-sized calvarial defects (Fig. 3c). The tissue architecture revealed that the bone had a lamellar pattern, contained viable osteocytes, and was rimmed with osteoblasts engaged in bone formation. There was no evidence of dystrophic calcifications. Osteocytes and osteoblasts were evident in the regenerated bone from samples treated with anti-BMP2 mAb alone, hBMMSCs alone, and rhBMP2 alone. On the other hand, histological analysis revealed that sites implanted with alginate loaded with non-specific isotype mAb (negative control) contained only fibrous and vascular connective tissue components consisting of interwoven bundles of collagenous fibers and unresorbed alginate hydrogel (Fig. 3c). Histomorphometric analysis indicated that hBMMSCs encapsulated in alginate with anti-BMP2 mAb formed significantly greater ( $p < 0.05$ ) amounts of mineralized tissue than either alginate-encapsulated hBMMSCs or non-specific isotype mAb, and indeed that the hBMMSC + anti-BMP2 mAb combination was able to repair the critical-sized defects (Fig. 3d). Quantitative analysis demonstrated significant improvement in the amount of bone regenerated by hBMMSCs and anti-BMP2 mAb together ( $p < 0.05$ ).

To further characterize MSC-mediated, antibody-assisted bone formation, we utilized immunohistochemical staining. The samples consisting of anti-BMP2 mAb absorbed to alginate encapsulating hBMMSC, anti BMP2-mAb alone, and alginate encapsulated hBMMSC revealed the shared capacity to attract and hold BMP2 ligands, as revealed by positive immunostaining (Fig 4a, upper panel). Not surprisingly, the samples treated with rh-BMP2 also revealed the presence of the BMP ligand, while the non-specific isotype mAb failed to trap the BMP2 ligand. We also performed semi-quantitative analysis for the presence of BMP2 ligand (see upper panel, Fig. 4a), which confirmed the attraction of endogenous BMPs by the mAb (Fig. 4b). Similarly, the positive controls and experimental samples revealed cells that express the bone transcription factor, Runx2, while the negative control (non-specific isotype mAb) did not. Finally, the human origin of the osteoblasts and

osteocytes was confirmed by their positive immunostaining with anti-human mitochondrion antibody when hBMMSCs were engrafted (Fig. 4a lower panel).

#### 4. DISCUSSION

Current treatment modalities for bone regeneration in craniofacial reconstructive surgeries and regenerative medicine more broadly consist of implantation with autogenous, allogeneic, xenogenic, and synthetic biomaterials. There are many disadvantages associated with autologous grafts, including a limited donor supply and the high rate of harvest morbidity. The advent of allografts, xenografts, and synthetic biomaterials has enabled clinicians to avoid some of the pitfalls associated with autografts; however, their efficacy is restricted due to their lack of osteoinduction, unpredictable graft resorption, and unfavorable mechanical properties [4-6]. A way of avoiding all of these materials and their drawbacks is suggested by the fact that BMPs have been identified as the major mediators in bone regeneration and formation. It is well known that exogenous administration of rhBMP2 can initiate a healing cascade that mediates bone regeneration through the TGF- $\beta$ /BMP signaling pathway [25,26].

Recombinant human bone morphogenetic protein 2 (rhBMP2) has been widely used for bone regenerative procedures, providing a promising alternative therapeutic option to autologous bone grafting. However, there are several disadvantages attributed to the application of rhBMP2. First, in order to be clinically effective, superphysiologic doses of the growth factor are needed. In addition, the inability to sustain growth factor concentration over extended periods of time leads to lower biological activity of recombinant BMP2. Compounding these issues, rhBMP2 is a very expensive therapeutic modality [27-29]. Therefore, alternatives to rhBMP2 are desirable. Recently, Freire *et al.* reported a bone regenerative therapy, in which anti-BMP2 monoclonal antibodies were capable of capturing endogenous BMP growth factors from the local host-graft site, with demonstrated efficacy in promoting bone repair and regeneration [20, 21]. Additionally, other studies have shown that a short treatment of MSCs with BMP2 ligand stimulated Runx-2 and osteopontin gene expression, leading to enhanced bone regeneration [30, 31]. Therefore, in this study, we developed an MSC delivery system that can be preloaded with anti-BMP2 mAb. We hypothesized that mesenchymal stem cells combined with antibodies against BMP2 could provide a promising platform for bone tissue engineering through capturing endogenous BMPs.

Using mesenchymal stem cells to regenerate bone comes with its own distinct set of advantages. The application of cell-delivery substrates, which provide a suitable microenvironment for tissue regeneration, is considered to be crucial for the complete repair of bony defects [32-34]. Biomaterial design has focused on controlling the material chemistry to direct cell and tissue responses and to promote highly specific binding interactions between the material and surrounding cells [35-37]. It has been reported that scaffolds seeded with appropriate MSCs can provide a suitable microenvironment with nutrients for prolonged cell viability and osteogenic potential, making this approach a promising treatment modality [38,39]. In our study, we sought to design an appropriate microenvironment by engineering the physicochemical properties of the extracellular MSC microenvironment in order to tailor the niche characteristics and direct cell differentiation and phenotype. To accomplish this, we developed an alginate hydrogel scaffold loaded with anti-BMP2 mAbs. Alginates are of particular interest for bone engineering applications due to their unique properties, including injectability and biodegradability [40,41]. Alginate can provide a 3D scaffold that facilitates the spatial distribution of MSCs, thus resulting in a structural organization that resembles the native *in vivo* microenvironment.



An injectable alginate-hydrogel microsphere loaded with anti-BMP2 mAb was developed and described here as a stem cell delivery system for potential application in bone tissue engineering. We showed the feasibility of applying hBMMSCs encapsulated in alginate hydrogel microspheres preloaded with anti-BMP2 mAb as a treatment modality for bone regeneration. This approach utilizes the regenerative potential of anti-BMP2 mAb to capture endogenous BMP2 and present it to MSCs. We confirmed through multiple independent methods that stem cell-mediated osteogenesis was indeed assisted by the mAb capturing endogenous BMP2. Micro-CT and histological analyses confirmed a significant increase in the amount of bone repair in the presence of a combination of hBMMSCs and anti-BMP2 mAb.

Our *in vitro* assay confirmed the presence of cross-reactivity between hBMMSC BMP receptors with the anti-BMP2mAb + rhBMP2 immune complex, while the non-specific isotype control mAb (Iso mAb) immune complex with rhBMP2 failed to bind to BMP receptors on the MSCs (due to unfavorable binding mode). We further investigated the molecular mechanism governing osteogenic differentiation of hBMMSCs in the presence of mAb in an *in vitro* model by developing a culture system to study this molecular mechanism. The data confirmed that bone regeneration is modulated by the BMP signaling pathway through the anti-BMP2 mAb capturing BMP2 ligands. In the presence of anti-BMP2 mAb, increased expression of the positive modulators of osteogenesis, p-Smad 1 and Runx2, was observed. These findings were well supported by biomineralization results reported by Alizarin red S staining showing that anti-BMP2 mAb + rhBMP2 immune complex successfully induced osteogenic differentiation of hBMMSCs, while hBMMSCs in the presence of non-specific isotype control mAb failed to do so.

We further demonstrated the possibility of enhancing the osteo-differentiation of hBMMSC encapsulated in alginate microspheres in the presence of anti-BMP2 mAb *in vivo*. When the encapsulated hBMMSCs were transplanted into critical-size calvarial defects in mice, they regenerated bone tissue to repair critical-sized defects that by definition would never repair without intervention. In addition, the osteoblasts and osteocytes within the newly-formed bone tissue expressed the osteogenic markers Runx2 and BMP2, as shown by immunodetection. As expected, in the presence of anti-BMP2 mAb, we observed a significant increase in the area that tested positive for BMP2 ligands. Furthermore, we confirmed the human origin of the cellular components of the bone tissue produced by the grafting hBMMSCs using specific antibodies against human mitochondria.

Based on our accumulated data, the efficacy of hBMMSC-mediated mAb-assisted bone regeneration can attributed to the ability of anti-BMP2 monoclonal antibody to capture endogenous BMP2 ligands and hence to direct differentiation of hBMMSCs toward osteogenic lineage through modulating the BMP signaling pathway.

## Conclusions

This study describes a technique for leveraging a system of mesenchymal stem cell-mediated, mAb-assisted bone regeneration. Here we describe a bone regeneration strategy based on *in vitro* and *in vivo* experiments which demonstrate the capacity of hBMMSCs to respond to the inductive signals provided by an anti-BMP2 mAb. We utilized the ability of anti-BMP2 mAb to trap and tether endogenous BMP2 ligands for the directed osteo-differentiation of hBMMSCs using an RGD-alginate microencapsulation system. The advantages of this system include its simplicity and ease with which it can be modified to encapsulate hBMMSCs in an injectable and biodegradable alginate hydrogel, yielding a 3-dimensional, cell delivery scaffold for bone tissue engineering.

## Acknowledgments

This work was supported by a grant from the National Institute of Dental and Craniofacial Research (R01 DE019932 to S.S and DE06988 to MLS). First authors (AM and SA) were supported by a NIDCR postdoctoral training grant (T90DE021982).

## References

1. Sachlos E, Czernuszka JT. Making tissue engineering scaffolds work. Review on the application of solid freeform fabrication technology to the production of tissue engineering scaffold. *Eur Cell Mater.* 2003; 5:29–40. [PubMed: 14562270]
2. Porter JR, Ruckh TT, Popat KC. Bone tissue engineering: a Review in Bone biomimetics and drug delivery strategies. *Biotechnol Prog.* 2009; 25:1539–1560. [PubMed: 19824042]
3. Monaco E, Bionaz M, Hollister SJ, Wheeler MB. Strategies for regeneration of the bone using porcine adult adipose-derived mesenchymal stem cells. *Theriogenology.* 2011; 75:1381–99. [PubMed: 21354606]
4. Betz VM, Betz OB, Harris MB, Vrahas MS, Evans CH. Bone tissue engineering and repair by gene therapy. *Front Biosci.* 2008; 13:833–841. [PubMed: 17981592]
5. Arrington ED, Smith WJ, Chambers HG, Bucknell AL, Davino NA. Complications of iliac crest bone graft harvesting. *Clin Orthop Relat Res.* 1996; 329:300–309. [PubMed: 8769465]
6. Kretlow JD, Young S, Klouda L, Wong M, Mikos AG. Injectable biomaterials for regenerating complex craniofacial tissues. *Adv Mater.* 2009; 21:3368–79. [PubMed: 19750143]
7. Hill E, Boonthekul T, Mooney DJ. Designing scaffolds to enhance transplanted myoblast survival and migration. *Tissue Eng Part A.* 2006; 12:1295–1302.
8. García-Gómez I, Elvira G, Zapata AG, Lamana ML, Ramírez M, Castro JG, et al. Mesenchymal stem cells: biological properties and clinical applications. *Expert Opin Biol Th.* 2010; 10:1453–1468.
9. Tasso R, Fais F, Reverberi D, Tortelli F, Cancedda R. The recruitment of two consecutive and different waves of host stem/progenitor cells during the development of tissue-engineered bone in a murine model. *Biomaterials.* 2010; 31:2121–2129. [PubMed: 20004968]
10. Chung IH, Yamaza T, Zhao H, Choung PH, Shi S, Chai Y. Stem cell property of post migratory cranial crest cells and their utility in alveolar bone regeneration and tooth development. *Stem Cells.* 2009; 27:866–877. [PubMed: 19350689]
11. Bueno EM, Glowacki J. Cell-free and cell-based approaches for bone regeneration. *Nat Rev Rheumatol.* 2009; 5:685–697. [PubMed: 19901916]
12. Liu Y, Wang L, Kikuri T, Akiyama K, Chen C, Xu X, et al. Mesenchymal stem cell-based tissue regeneration is governed by recipient T lymphocytes via IFN-gamma and TNF-alpha. *Nat Med.* 2011; 17:1594–1601. [PubMed: 22101767]
13. Liu J, Sato C, Cerletti M, Wagers A. Notch signaling in the regulation of stem cell self-renewal and differentiation. *Curr Top Dev Biol.* 2010; 92:367–409. [PubMed: 20816402]
14. Kratchmarova I, Blagoev B, Haack-Sorensen M, Kassem M, Mann M. Mechanism of divergent growth factor effects in mesenchymal stem cell differentiation. *Science.* 2005; 308:1472–1477. [PubMed: 15933201]
15. Czyz J, Wobus AM. Embryonic stem cell differentiation: the role of extracellular factors. *Differentiation.* 2001; 68:167–174. [PubMed: 11776469]
16. Chin M, Ng T, Tom W, Carstens M. Repair of alveolar clefts with recombinant human bone morphogenetic protein (rhBMP-2) in patients with clefts. *J Craniofac Surg.* 2005; 16:778–790. [PubMed: 16192856]
17. Khan S, Lane J. The use of recombinant human bone morphogenetic protein-2 (rhBMP-2) in orthopaedic applications. *Expert Opin Biol Th.* 2004; 4:741–753.
18. Wikesjo UM, Polimeni G, Qahash M. Tissue engineering with recombinant human bone morphogenetic protein-2 for alveolar augmentation and oral implant osseointegration: experimental observations and clinical perspectives. *Clin Implant Dent Relat Res.* 2005; 7:112–129. [PubMed: 15996358]

19. Zhu W, Rawlins BA, Boachie-Adjei O, Myers ER, Arimizu J, Choi E, et al. Combined bone morphogenetic protein-2 and -7 gene transfer enhances osteoblastic differentiation and spine fusion in a rodent model. *J Bone Miner Res.* 2004; 19:2021–2032. [PubMed: 15537446]
20. Freire MO, You HK, Kook JK, Choi JH, Zadeh HH. Antibody-mediated osseous regeneration: a novel strategy for bioengineering bone by immobilized anti-bone morphogenetic protein-2 antibodies. *Tissue Eng Part A.* 2011; 17:2911–2921. [PubMed: 21870943]
21. Freire MO, Kim HK, Kook JK, Nguyen A, Zadeh HH. Antibody-mediated osseous regeneration: the early events in the healing response. *Tissue Eng Part A.* 2013; 19:1165–74. [PubMed: 23190409]
22. Shi S, Gronthos S, Chen S, Reddi A, Counter CM, Robey PG, et al. Bone formation by human postnatal bone marrow stromal stem cells is enhanced by telomerase expression. *Nat Biotechnol.* 2002; 20:587–91. [PubMed: 12042862]
23. Moshaverinia A, Chen C, Akiyama K, Ansari S, Xu X, Chee WW, et al. Alginate hydrogel as a promising scaffold for dental-derived stem cells: an *in vitro* study. *J Mater Sci: Mater Med.* 2012; 23:3041–3051. [PubMed: 22945383]
24. Moshaverinia A, Chen C, Akiyama K, Xu X, Chee WW, Schricker SR, et al. Encapsulated dental-derived stem cells in an injectable and biodegradable scaffold for applications in bone tissue engineering. *J Biomed Mater Res Part A.* 2013 In Press.
25. Guo X, Wang XF. Signaling cross-talk between TGF-beta/BMP and other pathways. *Cell Res.* 2009; 19:71–88. [PubMed: 19002158]
26. Zhang YE. Non-Smad pathways in TGF- signaling. *Cell Res.* 2009; 19:128–139. [PubMed: 19114990]
27. Ishikawa H, Kitoh H, Sugiura F, Ishiguro N. The effect of recombinant human bone morphogenetic protein-2 on the osteogenic potential of rat mesenchymal stem cells after several passages. *Acta Orthop.* 2007; 78:285–296. [PubMed: 17464620]
28. Oldham J, Lu L, Zhu X, Porter B, Hefferan T, Larson D, et al. Biological activity of rhBMP-2 released from PLGA microspheres. *J Biomech Eng.* 2000; 122:289. [PubMed: 10923299]
29. Chen D, Zhao M, Mundy G. Bone morphogenetic proteins. *Growth Factors.* 2004; 22:233. [PubMed: 15621726]
30. Knippenberg M, Helder MN, Zandieh DB, Wuisman PI, Klein-Nulend J. Osteogenesis versus chondrogenesis by BMP-2 and BMP-7 in adipose stem cells. *Biochem Biophys Res Commun.* 2006; 342:902–908. [PubMed: 16500625]
31. Liu DD, Zhang JC, Zhang Q, Wang SX, Yang MS. TGF-β/BMP signaling pathway is involved in cerium-promoted osteogenic differentiation of mesenchymal stem cells. *J Cell Biochem.* 2013; 114:1105–14. [PubMed: 23150386]
32. Engler AJ, Sen S, Sweeney HL, Discher DE. Matrix elasticity directs stem cell lineage specification. *Cell.* 2006; 126:677–689. [PubMed: 16923388]
33. Valamehr B, Jonas SJ, Polleux J, Qiao R, Guo S, Gschwend EH, et al. Hydrophobic surfaces for enhanced differentiation of embryonic stem cell-derived embryoid bodies. *P Natl Acad Sci U S A.* 2008; 105:14459–14464.
34. Sapir Y, Kryukov O, Cohen S. Integration of multiple cell-matrix interactions into alginate scaffolds for promoting cardiac tissue regeneration. *Biomaterials.* 2011; 7:1838–47. [PubMed: 21112626]
35. Evangelista MB, Hsiong SX, Fernandes R, Sampaio P, Kong H, Barrias CC, et al. Upregulation of bone cell differentiation through immobilization within a synthetic extracellular matrix. *Biomaterials.* 2007; 28:3644–3655. [PubMed: 17532040]
36. Cantu DA, Hematti P, Kao WJ. Cell encapsulating biomaterial regulates mesenchymal stromal/stem cell differentiation and macrophage immunophenotype. *Stem Cell Transl Med.* 2012; 1:740–9.
37. Wang W, Ma N, Kratz K, Xu X, Li Z, Roch T, et al. The influence of polymer scaffolds on cellular behaviour of bone marrow derived human mesenchymal stem cells. *Clin Hemorheol Microcirc.* 2012; 52:357–73. [PubMed: 22975951]
38. Alsberg A, Anderson KW, Albeiruti A, Franceschi RT, Mooney DJ. Cell-interactive alginate hydrogels for bone tissue engineering. *J Dent Res.* 2001; 80:2025–2029. [PubMed: 11759015]

39. Hill E, Boontheekul T, Mooney DJ. Designing scaffolds to enhance transplanted myoblast survival and migration. *Tissue Eng Part A*. 2006; 12:1295–1302.
40. Rowley JA, Madlambayan G, Mooney DJ. Alginate hydrogels as synthetic extracellular matrix materials. *Biomaterials*. 1999; 20:45–51. [PubMed: 9916770]
41. Smidsrod O, Skjakbraek G. Alginate as immobilization matrix for cells. *Trends in Biotech*. 1990; 8:71–78.

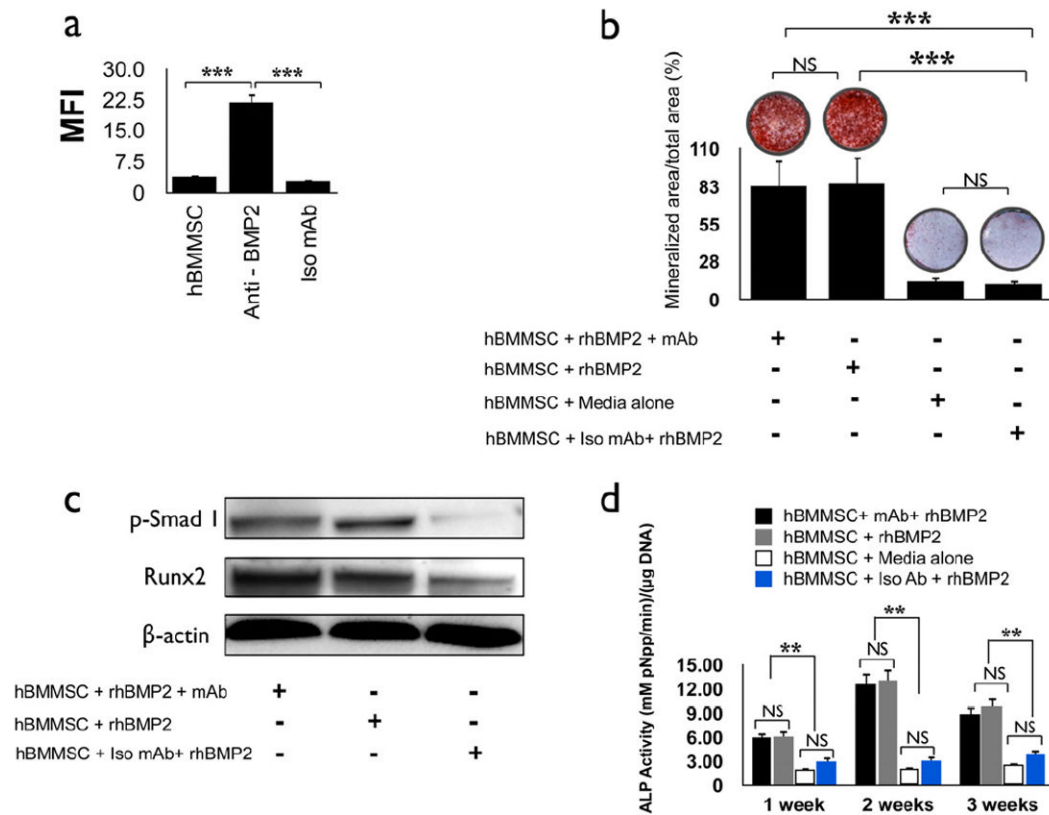


**Figure 1. Anti-BMP2 mAb + rhBMP-2 immune complex binds to BMP receptors on hBMMSCs and contributes to osteogenic differentiation of hBMMSCs in vitro**

(a) Analysis by flow cytometry of murine anti-BMP2 monoclonal antibody (mAb) immune complex bound to human recombinant BMP2 ligand (rhBMP2) interacting with the BMP receptors on hBMMSCs. The median fluorescent intensity (MFI) revealed binding between the immune complex with the BMP receptors located on the hBMMSCs. hBMMSCs alone and non-specific isotype mAb (Iso mAb) failed to reveal BMP2 ligand binding. (b) Qualitative and quantitative measurement for calcium ion localized to biomineralized nodule using Alizarin red S dye formed by hBMMSCs after treatment with either BMP2 ligand or anti-BMP2 mAb + rhBMP2 and cultured for two weeks. (c) Western blot analysis showing changes in the levels of expression of critical regulators of osteogenesis by hBMMSCs. The levels of phospho-Smad1 (p-Smad 1) and Runx2 transcription factor are elevated in hBMMSCs grown in the presence of anti-BMP2 monoclonal antibody + rhBMP2 or rhBMP2 ligand alone compared to cells maintained in the presence of non-specific isotype mAb (Iso mAb). (d) Alkaline phosphatase (ALP) activity for hBMMSCs in the presence or absence of anti-BMP2 mAb. The ALP value was normalized to the DNA concentration, with units of mM pNpp min<sup>-1</sup>/μg DNA. \**P*<0.05, \*\**P*<0.001, \*\*\**P*<0.001, n=5 for each group.

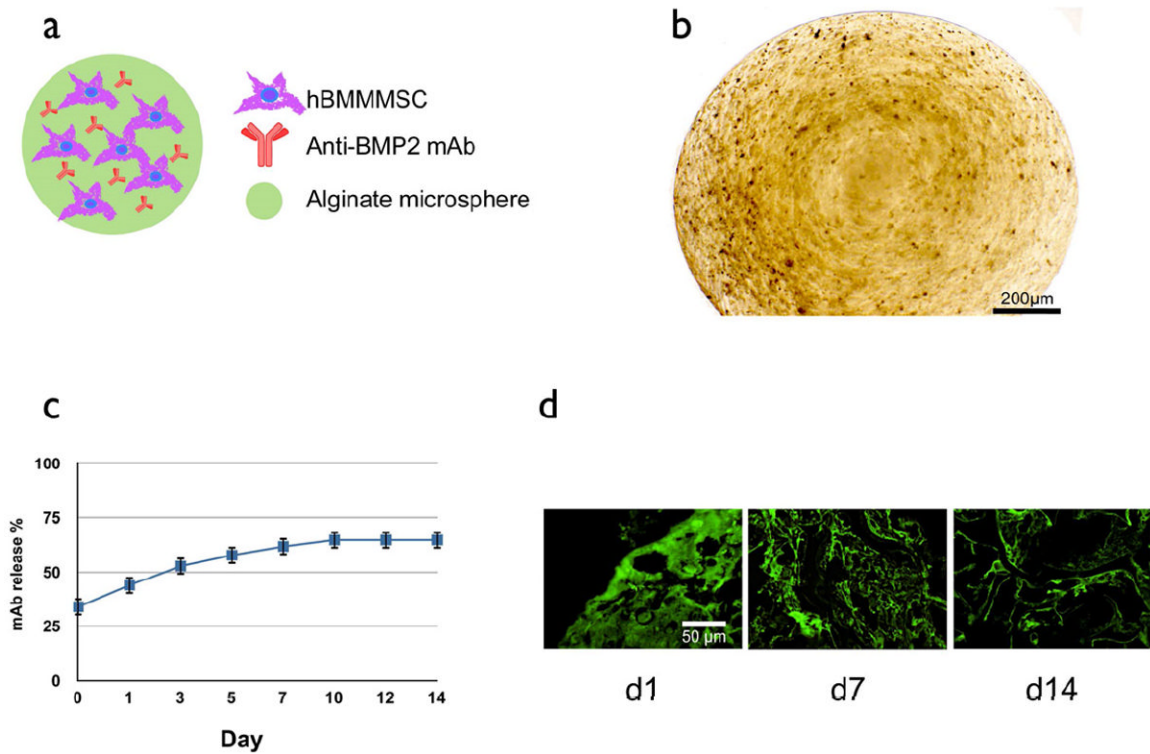


**Figure 2. Development of the hBMMSC microencapsulation system with sustained mAb release characteristics in vitro**

(a) Schematic presentation of the MSC-based co-delivery system containing anti-BMP2 mAb. (b) Bright field image of the alginate beads showing they retain their spherical shape with a uniform cell distribution (average capsule diameter  $1 \pm 0.1$  mm). (c) Characterization of the *in vitro* release profile of anti-BMP2 mAb-loaded alginate microspheres showing sustained release of anti-BMP2 mAb from alginate microspheres. mAb release is calculated from the total amount of anti-BMP2 mAb released after 14 days. (d) Confocal laser scanning microscopy analysis showing immobilized anti-BMP2 mAb (green signal) on microspheres after staining with FITC-conjugated goat anti-mouse secondary antibody and detected by confocal laser fluorescent microscopy showing that anti-BMP2 mAb is retained on the microspheres for up to two weeks *in vitro*.

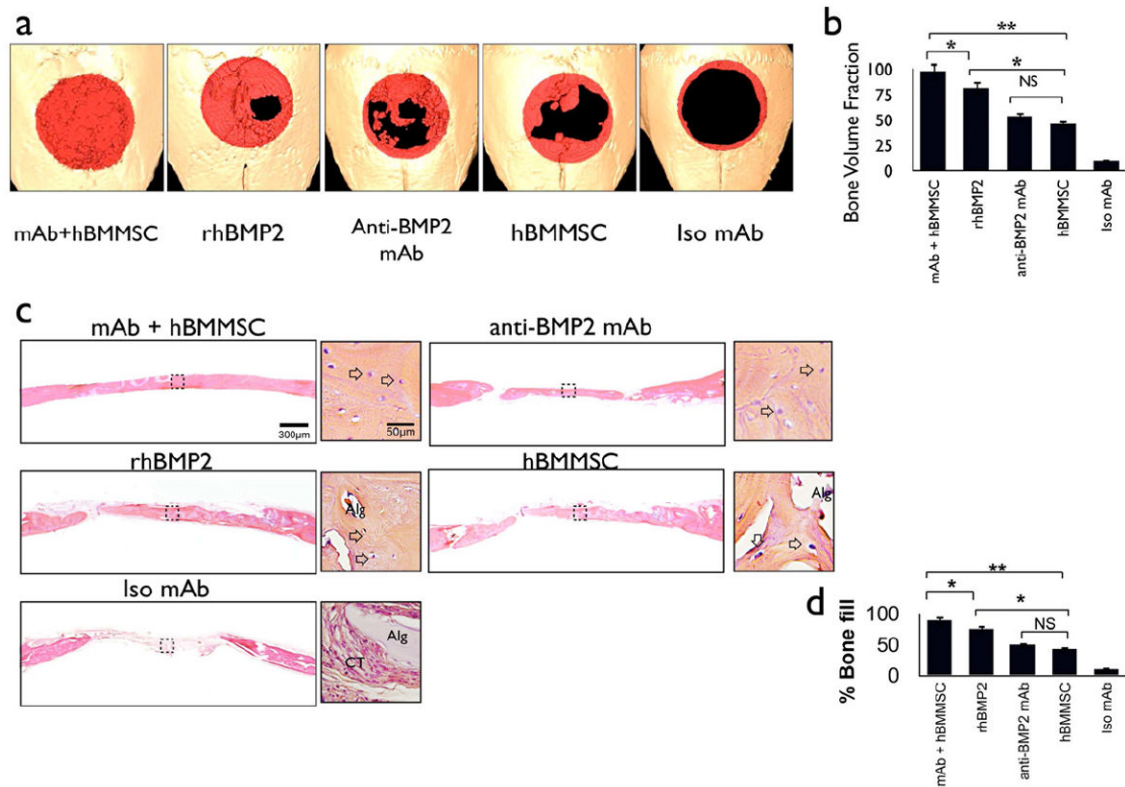


**Figure 3. hBMMSCs encapsulated in RGD-alginate microspheres loaded with anti-BMP2 mAb contribute to bone regeneration in a critical-size calvarial defect model**

(a) Micro-CT results of bone repair in mouse calvarial defects. Regenerated bone is pseudo-colored red. (b) Semi-quantitative analysis of bone formation based on micro-CT images; (c) Microanatomic representation of repair of critical-size defects in the mouse calvaria after 8 weeks of transplantation at high ( $\times 40$ ) and low ( $\times 4$ ) magnifications stained with H&E. Arrows point to osteocytes in lacunae (Alg: unresorbed alginate, CT: connective tissue). (d) Histomorphometric analysis of calvarial defects showing the relative amount of bone formation in the critical size calvarial defect model. \* $P < 0.05$ , \*\* $P < 0.01$ ,  $n = 4$  for each group.

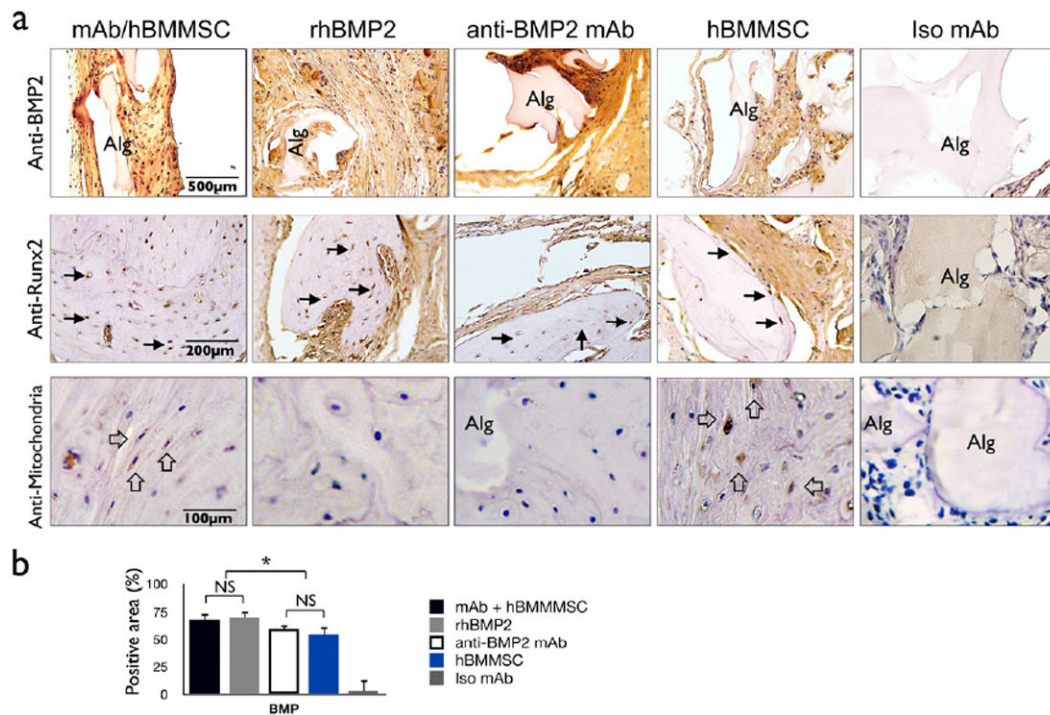


**Figure 4. Characterization of the origin and fate of MSCs after transplantation**

(a) Upper Panel: Cells and alginate positive for BMP2 epitopes are stained brown. Middle Panel: Cells expressing the bone-associated transcription factor Runx2 are stained brown (black arrows). Lower Panel: The human origin of the engrafted cells is confirmed by immunostaining with an antibody specific for human mitochondria (open arrows). Tissue formed in the negative control samples (e.g., non-specific isotype mAb [Iso mAb] failed to express either BMP2 or Runx2 and did not contain cells of human origin. (b) Semi-quantitative analysis of the percentage of cells and alginate positive for BMP2 protein taken from images shown in the upper panel of (a). \* $P < 0.05$ , \*\* $P < 0.01$ .